Modified carbon black/nylon 6 fibres with excellent antistatic and mechanical properties

Zhang Xin, Yin Shanshan, Meng Yang, Han Jian ✉, *Su Juanjuan*

Zhejiang Provincial Key Laboratory of Industrial Textile Materials and Manufacturing Technology, College of Materials and Textiles, Zhejiang Sci-Tech University, Hangzhou 310018, People's Republic of China
✉ *E-mail: hanjian8@zstu.edu.cn*

Published in Micro & Nano Letters; Received on 15th July 2019; Revised on 24th August 2019; Accepted on 18th September 2019

Nylon 6 (PA6) fibre has many advantages such as high strength, wear resistance, light weight, and good elasticity. However, PA6 fibre is prone to deformation in use and the antistatic ability is poor. In this Letter, the dispersion of carbon black (CB) was improved by physical methods and then added to the nylon 6 (PA6). The authors had studied that the dispersion of modified and unmodified CB in PA6 fibres with excellent mechanical properties and electrical conductivity. The results of Zeta potential and particle size test showed that the size of the CB particle modified was decreased and the absolute value of Zeta potential on the surface was increased. The results of scanning electron microscopy showed that the CB had a good dispersion in PA6; the results of thermogravimetric and Fourier transform infrared analysis showed that polystyrene sodium sulphonate was successfully coated on the surface of CB; when 5% modified CB was added in PA6 fibres, the mechanical properties of PA6 were hold up well. Interestingly, when 5% CB modified was added in PA6 fibres, the resistance of CB modified/PA6 fibre with excellent mechanical properties was reached up to 4.89×10^{11} Ω.

1. Introduction: There are a wide variety of polyamides such as polyamides 6 (nylon6, PA6) and polyamides 66 (nylon 66, PA66), which have the largest output and widely used [1–3]. In real word, polyamides fibre has become the engineering plastics with the largest consumption and the second largest synthetic fibre [4, 5]. Polyamides are gradually replacing copper, aluminium, steel and other metal materials in many fields. Moreover, it is widely used in textile, electronics industry, automotive industry, medical, construction industry, and so on. With the development of industry, the production and technical level of PA6 fibre are constantly improved, but its functionality is not enough to meet the requirements of the current situation [6, 7].

Furthermore, antistatic fibre, a wearable flexible material, is becoming more and more important in many fields. However, pure nylon6 fibre is an insulating material, which cannot transfer freely the charge. In a word, pure nylon6 fibre with insulation limits the application of clothing in the medical treatment, automobile industry, electronics, mechanical equipment, and other fields [8, 9]. Importantly, if the static electricity has not been discharged in time, it will produce easily electric shock even explosion. Santos *et al.* [10] produced PA6/PAni nanofibre mats employing the electrospinning technique. The PA6/PAni nanofibre mat shows an electrical conductivity of 1.2×10^{-14} S/cm after 12% PAni was put into PA6. Scaffaro *et al.* [11] prepared PA6/carbon nanotube (CNT) fibres using the method of melt spinning. They found that the PA6/2wt.% CNT fibres have no conductivity. Therefore, the study of antistatic nylon 6 fibres is important in use.

Many methods are improving the electrical conductivity by adding the carbon black (CB) [12, 13]. CB is easy to obtain and low cost. However, the dispersiveness of CB is worse, because it has a high surface energy and high surface area, thus a super dispersed CB is the best choice to enhance the dispersity of CB and improve the antistatic electricity and mechanical properties of polymeric materials [14, 15]. Herein, we prepared PA6/CB fibres by melt spinning [16, 17]. In order to obtain a super dispersed CB and add into PA6 matrix, the CB was modified with polystyrene sodium sulphonate (PSS; average molecular weight 70,000) before polymerisation, enhancing the affinity with PA6 molecular chain and achieve the purpose of uniform dispersion. We have performed the test for the PA6/CB fibres by using the dynamic light scattering, thermogravimetric (TG), scanning electron microscopy (SEM), Fourier infrared spectroscopy (FTIR) and electrical resistance test [18–20].

2. Experimental

2.1. Materials: CB (Vulcan XC-72) was purchased from Carbot Corporation, USA. PA6, spinning level (Yiwu Huading Nylon Co., Ltd). Deionised water, formic acid, and sodium chloride were purchased from Hangzhou Gaojing Fine Chemical Co., Ltd. PSS was provided by Wengjiang Reagent.

2.2. Preparation of super dispersed CB: As shown in Figs. 1*a* and *b*, CB, PSS, and NaCl were firstly added to the beaker according to the mass ratio of 2:1:1, and then deionised water was mixed to the beaker. Furthermore, the above solution was stirred for 1–2 h at room temperature. Next, the products were washed with deionised water and dried at 60°C. Finally, a super dispersed CB was obtained, which is denoted as G-CB.

2.3. Preparation of PA6/G-CB fibre and PA6/CB fibre: PA6 was placed in a vacuum oven and dried at 80°C for 24 h. The mass ratio of PA6 and modified CB was 100:0, 95:5, 90:10 into the mixer (Fig. 1*c*). Next, in Fig. 1*e*, the products cut into small pieces seen from Fig. 1*d* were prepared in nascent PA6/G-CB (0, 5, 10%) fibre by the melt spinning under 250°C using a tiny spinning machine (HAAKE MiniLab II type, Germany's fly the world's science and technology company). Then, after the action of drawing roller, the nascent PA6/G-CB fibre was drafted four times in thermal drafting device (DSM XPLORE, Netherlands DSM Company) set at 120°C. Finally, the PA6/G-CB fibre was successfully prepared by the process in Figs. 1*e* and *f*. In the meantime, the method used to prepare PA6/CB (0, 5, and 10%) fibre was the same as that of PA6/G-CB (0, 5 and 10%) fibre.

2.4. Measurements: *Dispersion test*: The dispersion solution was prepared by the CB and G-CB in water and formic acid. The dispersion solution was stationary for 24 h to observe the stability of the dispersion solution.

The zeta potential and particle size of CB before and after modified was tested by laser dynamic light scattering instrument

doi: 10.1049/mnl.2019.0433

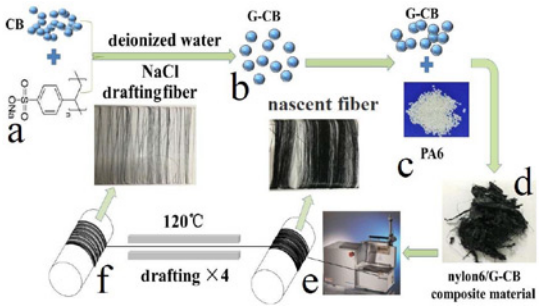

Fig. 1 *Preparation process of G-CB and PA6/G-CB fibre*
a Preparation of G-CB
b Modified carbon black
c Melt blending
d CB, G-CB and PA6 composites
e Spinning
f Draft (×4)

(LB-500 V) from Horiba Company, UK. Each sample was measured three times; the zeta potential and particle size were reported as an average value.

Fourier transform infrared spectrometer (FTIR, 5700) from Nicolet Company (USA) was used to analyse the molecular structure before and after the modification. In this experiment, potassium bromide tablet was used with a resolution of 4 cm^{-1}, a test range of 4000–500 cm^{-1}, and a scanning frequency of 64 times.

PA6/CB and PA6/G-CB fibres, the fracture structure and morphology were observed, and the dispersion of CB and G-CB were observed by using a UItra55 thermal field emission scanning electron microscope from Germany. The scanning voltage was 3 kV.

TG analyser (PYRIS1) was used to analyse the G-CB. Nitrogen gas velocity of 20 ml/min, the temperature range was 25–750°C, 10°C /min.

The fibres were with a length of 2 cm. Also, the szt-2a electrical conductivity tester (Jiangsu Suzhou Lattice Electronics Co., Ltd) was used. The electrical resistance of the samples was tested and the electrical conductivity of the PA6/CB and PA6/G-CB was analysed.

The mechanical properties of PA6/CB and PA6/G-CB fibres, INSTRON multifunctional testing machine was used to conduct tensile tests on materials with a tensile speed of 20 mm/min and a clamping distance of 2 cm to obtain the mechanical properties of each material for comparison.

3. Results and discussion

3.1. Characterisation of G-CB and CB: Firstly, the dispersion of CB was observed by a sedimentation test with different solvents (deionised water and formic acid). Secondly, the results of settlement experiments were further verified by an optical microscope. The results are shown in Figs. 2 and 3.

As can be seen from Fig. 2, after 24 h of sedimentation experiment, CB was settled obviously in deionised water, and the upper

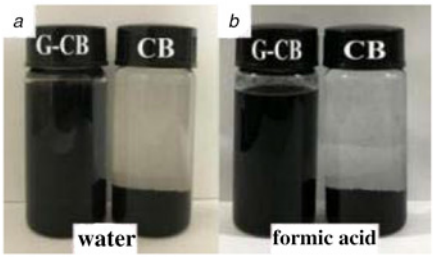

Fig. 2 *G-CB and CB dispersion test*
a Dispersion of G-CB and CB in water
b Dispersion of G-CB and CB in formic acid

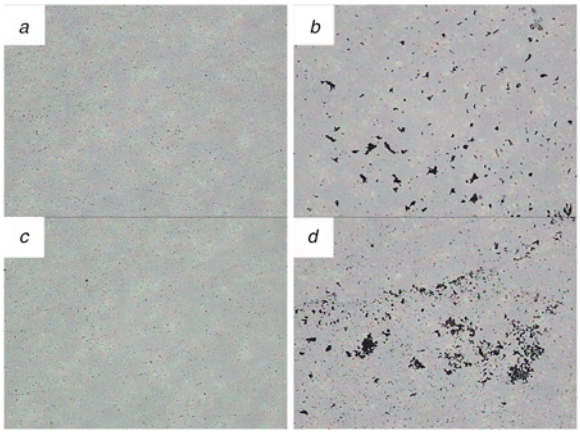

Fig. 3 *G-CB and CB dispersion optical microscope test*
a Optical micrograph of G-CB dispersed in water (×400)
b Optical micrograph of CB dispersed in water (×400)
c Optical micrograph of G-CB dispersed in formic acid (×400)
d Optical micrograph of CB dispersed in formic acid (×400)

layer was almost transparent. The G-CB was not stratified and has uniform colour. When formic acid was used as solvent, CB was settled obviously after 24 h. After modification, G-CB was dispersed evenly in formic acid solution without settling and stratification, indicating that the dispersiveness of CB was significantly improved after modification of PSS. Moreover, in Fig. 3, the results prove that G-CB was dispersed evenly in water and formic acid compared to the agglomeration of CB. In short, the above results have shown that PSS has successfully modified CB.

The results of zeta potential and particle size are shown in Table 1. It could be concluded from the table that the zeta potential of CB and the absolute value of zeta potential was relatively weak, which was because the CB with the high surface energy generates aggregation. Meanwhile, the dispersion system of G-CB was uniform compared to CB.

The absolute value of zeta potential for CB modified was significantly increased from 9.12 to 19.50 mV, and the corresponding particle size was also reduced from 271.9 to 234.3 nm. According to the theory of double electric layer [21], the absolute value of zeta potential was greater, and the electrostatic repulsion was greater. The reason was that CB coated by PSS was mostly presented as small aggregates, which resulted in excellent electrostatic repulsive force and dispersion stability. The above results were consistent with that of sedimentation experiments and optical microscope tests.

The infrared spectra of CB and G-CB are shown in Fig. 4. It can be seen from Fig. 4*a* that absorption peaks of CB appeared at 3440 cm^{-1} and 1630 cm^{-1} before modification, which were the bending vibration peaks of –OH group and O–H (H_2O), respectively. The presence of these oxygen-containing functional groups provided the reaction sites for PSS to cover CB. The peaks of the G-CB became wider and steeper between 3000 cm^{-1} and 3600 cm^{-1}, which was due to the stretching vibration of C–H of benzene ring at 3100 cm^{-1}. The stretching vibration peaks of methyl and methylene groups were from 2800 to 2900 cm^{-1}. The 1450 cm^{-1} was the saturated C–H deformation vibration absorption peak. The 1300 and 1250 cm^{-1} were the stretching vibrations of the double bond S=O in PSS. From the above results, it could be concluded that after the modification

Table 1 Zeta potential and particle size of CB and G-CB

Sample	Zeta potential, mV	Particle size, nm
CB	−9.12	271.9
G-CB	−19.50	234.3

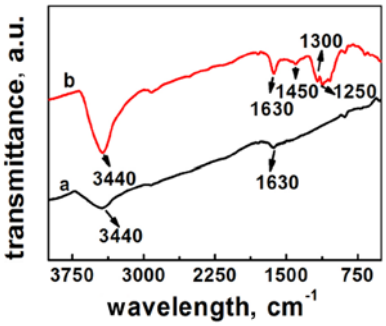

Fig. 4 *FTIR spectra of*
a CB
b G-CB

and preparation process, PSS had been successfully coated on the surface of CB, which proved that CB had been modified.

TG analysis of CB and G-CB was carried out to observe that PSS has been coated on the CB surface. According to the curves in Fig. 5, the curve of CB could be divided into three parts for analysis. The first part was 0–110°C, both mass losses, mainly the evaporation of water. In the second stage at 280–420°C, mainly due to the mass loss caused by the decomposition of some oxygen-containing functional groups on the surface of CB. The third part was 450–720°C. At this stage, there was almost no loss of CB, indicating that only pure CB exists in the CB at the time, and no other groups exist. The G-CB decreased slightly at 110–450°C. It was mainly the CB coated by PSS that causes the melting of PSS and slight loss at high temperature. However, the G-CB had a large loss at 450–720°C, mainly because PSS begins to decompose at this temperature, leaving only inorganic particles of CB. TG curves of CB and G-CB could be obtained. CB had been coated by PSS, and the coverage reached 4.46%.

From Fig. 6, we could see that the dispersion of CB was extremely poor. The agglomeration between particles was extremely serious. Also, the agglomeration exists in layers, which was found at high magnification. While CB modified by PSS showed obvious improvement in dispersion, and the particles were evenly dispersed without stacking. At high magnification, it was also found that the particle stacking was obviously decreased and the dispersion of G-CB was obviously improved. It could be preliminarily known from the results of SEM that PSS had successfully modified CB and improved the dispersion of CB.

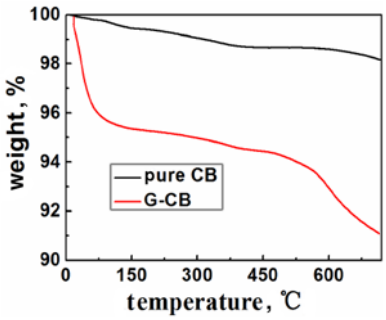

Fig. 5 *TG curves of CB and G-CB*

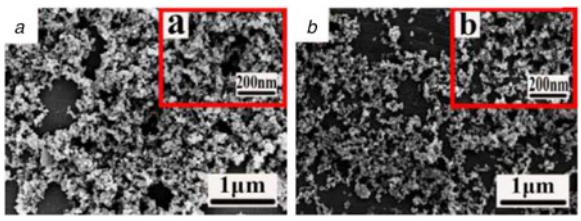

Fig. 6 *Micrograph of*
a CB
b G-CB

3.2. Characterisation of PA6/G-CB fibre and PA6/CB fibre: INSTRON multifunctional testing machine was used to test the mechanical properties of the materials, and the test results are shown in Fig. 7*a*. Compared with pure PA6 fibre, the mechanical properties of other fibres were reduced. However, it is worth noting that the tensile strength and strain of PA6/5% G-CB fibre was higher than the PA6/5% CB-fibre. Similarly, when the content of CB and G-CB was 10%, the tensile strength and strain of PA6/G-CB fibre were higher than the PA6/CB fibre. The results show that G-CB can improve the mechanical properties of PA6 fibre, in contrast, to add pure CB in the PA6 fibre. More specifically, in Fig. 7*b*, when the content of G-CB was 5% in PA6 fibre, the tensile strength was increased to 293 MPa compared to PA6/5% CB fibre (274 MPa). Moreover, when the content of G-CB was 10% in PA6 fibre, the tensile strength was weakly decreased to 132 MPa in contrast to PA6/10% CB fibre (40 MPa). Compared with pure PA6 fibre, the tensile strength of PA6/5% G-CB fibre had decreased by 9.56%. The tensile strength of PA6/10% G-CB fibre was reduced by 59.26%. The tensile strength of PA6/5% CB fibre decreased by 15.43%, while that of PA6/10% CB fibre decreased by 87.65%. The reason was that the CB exhibited the phenomenon of large aggregates and poor

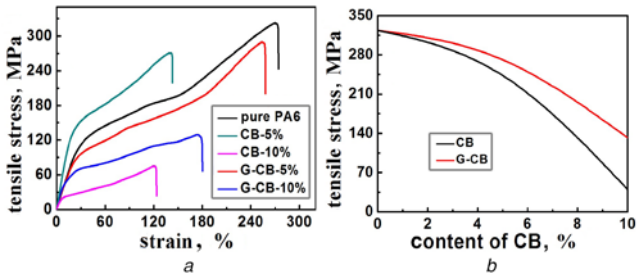

Fig. 7 *Mechanical property test of composite fibre*
a Tensile stress–strain curves of pure PA6 fibre, PA6/CB, and PA6/G-CB fibre
b Tensile stress of PA6/CB and PA6/G-CB fibre in different contents of CB and G-CB

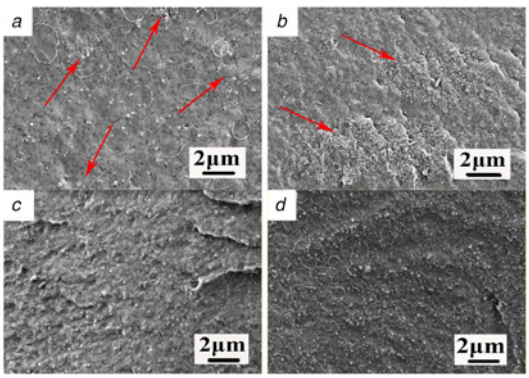

Fig. 8 *Electron micrograph of the cross section of the composite fibre*
a Cross section of PA6/5% CB fibre
b Cross section of PA6/10% CB fibre
c Cross section of PA6/5% G-CB fibre
d Cross section of PA6/10% G-CB fibre

doi: 10.1049/mnl.2019.0433

Table 2 Resistance and conductivity of PA6, PA6/ CB, and PA6/G-CB fibres

Sample	Diameter Φ, mm	Resistance, Ω	Electrical resistivity ρ, Ω cm	Electrical conductivity σ, S/cm
pure PA6	0.06	1.30×10^{15}	1.84×10^{12}	5.44×10^{-13}
5% CB	0.06	3.61×10^{13}	5.10×10^{10}	1.96×10^{-11}
10% CB	0.10	8.01×10^{11}	3.15×10^{9}	3.18×10^{-10}
5% G-CB	0.11	4.89×10^{11}	2.32×10^{9}	4.30×10^{-10}
10% G-CB	0.10	4.70×10^{10}	1.85×10^{8}	5.42×10^{-9}

compatibility in PA6 fibres, which resulted in heterogeneity of CB in PA6 fibres during spinning. As a result, when PA6/CB fibres were stretched, the aggregates of CB became concentration point of stress, and then resulted in fracture. At the same time, it was found that with the addition of CB, the agglomeration of CB became more serious and the mechanical properties were significantly decreased. With the addition of CB coated by PSS, there were small aggregates due to the increase of mutual repulsion. Meanwhile, the coating of PSS improved the compatibility with PA6. Therefore, G-CB could be more evenly dispersed in PA6 fibres. The results showed that the mechanical properties of PA6/ G-CB fibres were not significantly reduced. It was because the uniform dispersion of PSS-CB and the excellent compatibility with PA6. The results showed the mechanical properties of PA6/ G-CB fibres were improved, and the mechanical properties of PA6/G-CB fibres were significantly better than that of PA6/CB fibres under the same content. In a word, the tensile test results showed that the modified CB could improve the mechanical properties of the PA6 fibre.

The cross-sections of PA6/5% CB fibre, PA6/10% CB fibre, PA6/5% G-CB fibre and PA6/5% G-CB fibre were observed by SEM. The results of cross-sections in Figs. 8*a*–*d* proved further the reason for mechanical properties changed in PA6 fibre, PA6/CB fibre, and PA6/G-CB fibre. As shown in Figs. 8*a* and *b*, PA6/5%-CB fibre and PA6/10%-CB fibre exhibited rough cross-section denoted by red arrows owing to CB agglomerated with poor dispersibility into the PA6 matrix. In contrast, there was a good dispersibility of G-CB in the PA6 matrix of Figs. 8*c* and *d*, indicating that G-CB improved incompatible and agglomeration of pure CB in the PA6 matrix. For the PA6 matrix, all in all, SEM of cross-sections recorded that the dispersion of CB modified by PSS was greatly improved compared to the pure CB.

The length of PA6, PA6/CB, and PA6/G-CB fibres were 2 cm, and the diameter was measured by a thickness meter. The results are shown in Table 2.

The conductivity and resistivity of each fibre could be calculated by formula (1) and (2) [22]

$$R = \frac{\rho L}{s} \tag{1}$$

$$\sigma = \frac{1}{\rho} \tag{2}$$

where R is the resistance of the material, ρ is the electrical conductivity of the material, s is the cross-sectional area of the material, L is the length of the material, and σ is the electrical conductivity of the material.

As could be seen from the data in Table 2, it proved the insulation property of pure PA6 fibre, and the conductivity was low. After G-CB added, the electrical conductivity of the PA6/10% G-CB fibre was significantly increased to 5.42×10^{-9} S/cm and the resistance was significantly lower than that of the pure PA6 fibre. Significantly, when the content of G-CB was 5%, the PA6/G-CB fibre still has antistatic properties. This was because G-CB evenly distributed in PA6 matrix, which was well proved by SEM results, while CB had high surface energy, resulting in the obvious reunion of CB in PA6. Therefore, compared to PA6/ CB fibre, CB coated by PSS could form continuous conductive path in the PA6 matrix, which resulted in low resistivity of PA6/G-CB fibre. Compared with PA6/CB fibre and pure PA6 fibre, this work found that the resistance of PA6/G-CB fibre was weakly reduced. In a word, it is important to point out the theory that CB modified by PSS can be evenly dispersed in PA6 matrix because PSS reducing the surface energy of CB improves the compatibility between CB and PA6 matrix.

4. Conclusion: In order to obtain excellent antistatic and mechanical properties of PA6 fibres, PA6/G-CB fibre was prepared by the melt spinning. In the study, PSS was coated on surface of CB through physical modification, improving its dispersion and compatibility in the PA6 matrix, which is proved by FTIR, Zeta, TG, and SEM. Furthermore, in terms of these fibres as prepared, the PA6/G-CB fibre had good antistatic and mechanical properties compared to that of PA6/CB fibre when the content of G-CB was 5%. More significantly, mechanical properties of PA6/5% G-CB fibre were similar to that of PA6 fibre, improving the application value of PA6/G-CB fibre. Therefore, this work can provide two prospects that antistatic PA6/G-CB fibre yield a prospective value in use and ultra-dispersed CB is promisingly used in the automotive industry, electronics, mechanical equipment, and other fields.

5 References

[1] Wang X., Zheng Q., Yang G.: 'Influence of preparation methods on structure and properties of PA6/PA66 blends: a comparison of melt-mixing and in situ blending', *J. Polym. Sci. B, Polym. Phys.*, 2007, **45**, (10), pp. 1176–1186

[2] Isabel C., Elduque D., Santolaria J., *ET AL.*: 'The influence of environmental conditions on the dimensional stability of components injected with PA6 and PA66', *Polym. Test.*, 2015, **50**, pp. 15–25

[3] Ma Y., Zhou T., Su G., *ET AL.*: 'Understanding the crystallization behavior of polyamide6/polyamide66 alloys from the perspective of hydrogen bonds: projection moving-window 2D correlation FTIR spectroscopy and the enthalpy', *RSC Adv.*, 2016, **6**, (90), pp. 87405–87415

[4] Zhu X.D., Zang C.G., Jiao Q.J.: 'High electrical conductivity of nylon 6 composites obtained with hybrid multiwalled carbon nanotube/carbon fiber fillers', *J. Appl. Polym. Sci.*, 2014, **131**, (20), pp. 1–10

[5] Evans G.C., Desbois P., Lesser A.J.: 'Engineering impact modification of anionically polymerized polyamide 6', *J. Appl. Polym. Sci.*, 2018, **135**, (47), pp. 1–17

[6] Straat M., Rigdahl M., Hagstrom B.: 'Conducting bicomponent fibers obtained by melt spinning of PA6 and polyolefins containing high amounts of carbonaceous fillers', *J. Appl. Polym. Sci.*, 2012, **123**, (2), pp. 936–943

[7] Alisa Š., Jelena V., Andrej D., *ET AL.*: 'Polyamide 6 composite fibers with incorporated mixtures of melamine cyanurate, carbon nanotubes, and carbon black', *J. Appl. Polym. Sci.*, 2018, **136**, (5), pp. 1–11

[8] Cheng H.K.F., Sahoo N.G., Pan Y., *ET AL.*: 'Complementary effects of multiwalled carbon nanotubes and conductive carbon black on polyamide 6', *J. Polym. Sci. B, Polym. Phys.*, 2010, **48**, (11), pp. 1203–1212

[9] O'Neill A., David B., Brendan D., *ET AL.*: 'Preparation and properties of polyamide 6 nanocomposites covalently linked with amide functional graphene oxide', *J. Thermoplast. Compos. Mater.*, 2018, **31**, (2), pp. 162–180

[10] Santos J.P.F., Arjmand M., Melo G.H.F., *ET AL.*: 'Electrical conductivity of electrospun nanofiber mats of polyamide 6/polyaniline coated with nitrogen-doped carbon nanotubes', *Mater. Des.*, 2018, **141**, pp. 333–341
[11] Scaffaro R., Maio A., Tito A.C.: 'High performance PA6/CNTs nanohybrid fibers prepared in the melt', *Compos. Sci. Technol.*, 2012, **72**, (15), pp. 1918–1923
[12] Zabegaeva O.N., Sapozhnikov D.A., Buzin M.I., *ET AL.*: 'Nylon-6 and single-walled carbon nanotubes polyamide composites: formulation and characterization', *High Perform. Polym.*, 2017, **29**, (4), pp. 411–421
[13] Xiang M., Li C., Ye L.: 'Structure and conformation of polyether amine in confined space of graphene oxide and its enhancement on the electrically conductive properties of monomer casting nylon-6', *Compos. A, Appl. Sci. Manuf.*, 2017, **95**, pp. 1–11
[14] Dasari A., Yu Z.Z., Mai Y.W.: 'Electrically conductive and supertough polyamide-based nanocomposites', *Polymer*, 2009, **50**, (16), pp. 4112–4121
[15] Koysuren O., Yesil S., Bayram G.: 'Effect of surface treatment on electrical conductivity of carbon black filled conductive polymer composites', *J. Appl. Polym. Sci.*, 2007, **104**, (5), pp. 3427–3433
[16] Beom-Gon C., Seonghwan L., Sang-Ha H., *ET AL.*: 'Influence of hybrid graphene oxide-carbon nanotube as a nano-filler on the interfacial interaction in nylon composites prepared by in situ interfacial polymerization', *Carbon*, 2018, **140**, pp. 324–337
[17] Dencheva N., Gaspar H., Filonovich S., *ET AL.*: 'Fullerene-modified polyamide 6 by in situ anionic polymerization in the presence of PCBM', *J. Mater. Sci.*, 2014, **49**, (14), pp. 4751–4764
[18] Koysuren O., Yesil S., Bayram G.: 'Effect of composite preparation techniques on electrical and mechanical properties and morphology of nylon 6 based conductive polymer composites', *J. Appl. Polym. Sci.*, 2006, **102**, (3), pp. 2520–2526
[19] Nilsson E., Rigdahl M., Hagstrom B.: 'Electrically conductive polymeric bi-component fibers containing a high load of low-structured carbon black', *J. Appl. Polym. Sci.*, 2015, **132**, (29), pp. 1–9
[20] Lim S.J., Lee J.G., Hur S.H.: 'Effects of MWCNT and nickel-coated carbon fiber on the electrical and morphological properties of polypropylene and polyamide 6 blends', *Macromol. Res.*, 2014, **22**, (6), pp. 632–638
[21] Ridaoui H., Jada A., Vidal L., *ET AL.*: 'Effect of cationic surfactant and block copolymer on carbon black particle surface charge and size', *Colloids Surf. A, Physicochem. Eng. Aspects*, 2006, **278**, (1–3), pp. 149–159
[22] Zhang Q., Xiong H., Yan W., *ET AL.*: 'Electrical conductivity and rheological behavior of multiphase polymer composites containing conducting carbon black', *Polym. Eng. Sci.*, 2010, **48**, (11), pp. 2090–2209

doi: 10.1049/mnl.2019.0433